

OPEN

Toll-Like Receptor 3 Is Critical to the Pancreatic Islet Milieu That Is Required for Coxsackievirus B4–Induced Type 1 Diabetes in Female Nonobese Diabetic Mice

Sarah E. Benner, PhD,*† Debra L. Walter, PhD,*† Jean R. Thuma, MS,‡ Maria Courreges, PhD,‡ Calvin B. L. James, PhD,*§|| Frank L. Schwartz, MD,‡|| and Kelly D. McCall, PhD*†‡§||

Objective: Genetic and environmental influences play a role as triggers of type 1 diabetes mellitus (T1DM). Female nonobese diabetic (NOD) mice are useful for studying T1DM as they spontaneously develop T1DM, which can be accelerated by some viruses. Toll-like receptor 3 (TLR3) is believed to play a critical role in viral-induced T1DM and β -cell destruction, because female *Tlr3* knockout (*Tlr3*^{-/-}) NOD mice are protected from Coxsackievirus B4 (CVB4)-induced acceleration of T1DM. However, the exact role(s) TLR3 plays in the pathogenesis of CVB4-induced T1DM remain unknown.

Methods: This longitudinal study used immunostaining, laser capture microdissection, and reverse transcription real-time polymerase chain reaction of islets from female uninfected and CVB4-infected *Tlr3*^{+/+} and *Tlr3*^{-/-} NOD mice.

Results: Islets isolated from female *Tlr3*^{+/+} NOD mice 4 to 8 weeks of age had higher amounts of insulinitis, *Cxcl10*, *Il1b*, *Tnfa*, and *Tgfb1* expression compared with *Tlr3*^{-/-} NOD mice. After CVB4 infection, *Tlr3*^{+/+} NOD mice had higher amounts of insulinitis and T-cell infiltration at 3 days after infection compared with *Tlr3*^{-/-} CVB4-infected NOD mice.

Conclusions: Toll-like receptor 3 is necessary for establishment of a pancreatic islet inflammatory microenvironment by increasing insulinitis and cytokine expression that facilitates CVB4-induced T1DM in female NOD mice.

Key Words: immunohistochemistry, RT-qPCR, insulin, CD3, insulinitis, mouse models

(*Pancreas* 2022;51: 48–55)

Type 1 diabetes mellitus (T1DM) is an autoimmune disorder marked by destruction of insulin-producing β cells by one's own immune system and/or by an environmental insult. Both genetic and environmental factors play a role in the onset of T1DM, with considerable evidence that suggests viruses are one of the

key players.^{1–22} Specifically, coxsackie B viruses (CVBs), which are positive single-stranded RNA viruses, have been shown to trigger T1DM in susceptible individuals and in mouse models^{4,9,17,19,23–26}; however, the exact mechanisms by which CVBs trigger T1DM onset have yet to be elucidated.

In mammals, one of the mechanisms through which viruses are recognized is via toll-like receptors (TLRs), a specific class of innate immune receptors responsible for recognizing particular pathogen-associated and/or damage-associated molecular patterns (ie, PAMPs and DAMPs, respectively), such as viral double-stranded RNA (dsRNA), and eliciting an innate immune response.²⁷ In particular, toll-like receptor 3 (TLR3), which recognizes dsRNA, is known to be present in both immune and nonimmune cells, particularly in β cells of both the human and murine pancreas.^{27,28} Toll-like receptor 3 is responsible for recognizing both viral dsRNA and endogenous dsRNA released from damaged or dying host cells^{29–31} and signaling activation results in the production of type 1 interferons, inflammatory cytokines, and chemokines, and can lead to β -cell apoptosis.^{29,31–34} Previous reports show that when left in a sterile environment, female *Tlr3*^{-/-} nonobese diabetic (NOD) mice will develop T1DM at a similar rate as female *Tlr3*^{+/+} NOD mice.^{23,32} However, when a preexisting mass of autoreactive T cells is present within pancreatic islets, that is, after a “critical threshold” of insulinitis has been reached (ie, usually by 8 weeks of age),⁴ and then female *Tlr3*^{+/+} NOD mice are infected with CVB4, they rapidly develop T1DM.^{4,17,23,26} In contrast, female *Tlr3*^{-/-} NOD mice are protected from this viral acceleration of T1DM,²³ indicating that TLR3 is key for viral acceleration of T1DM in female NOD mice. Thus, although TLR3 is key to CVB4 acceleration of T1DM in female NOD mice, the mechanism(s) by which TLR3 mediates viral acceleration of T1DM in female NOD mice remains elusive. Herein, we used female *Tlr3*^{+/+} and *Tlr3*^{-/-} NOD mice to offer the first direct line of evidence to explain how TLR3 is involved in the establishment of the “critical threshold” of insulinitis that is permissive for CVB4-induced acceleration of T1DM in female NOD mice and how TLR3 affects a specific inflammatory islet environment 3 days after CVB4 infection.

MATERIALS AND METHODS

Animal Husbandry/Glucose Measurements/CVB4 Infection

This work was conducted with approval from the Ohio University Institutional Animal Care and Use Committee in accordance with accepted standards of humane animal care. Three-week-old female *Tlr3*^{+/+} NOD mice were obtained from the Jackson Laboratory (Bar Harbor, Maine) and housed in a sterile/germ-free facility. Breeding pairs of *Tlr3*^{-/-} NOD mice were kindly provided by Dr Li Wen (Yale University), and animals were generated as previously described.³² *Tlr3*^{-/-} NOD mice used in this study were from our breeding colony of these mice at Ohio

From the *Molecular and Cellular Biology Program, and †Department of Biological Sciences, Ohio University College of Arts & Sciences; Departments of ‡Specialty Medicine, §Biomedical Sciences, and ||Diabetes Institute, Ohio University Heritage College of Osteopathic Medicine, Athens, OH.

Received for publication March 15, 2021; accepted December 8, 2021.

Address correspondence to: Kelly D. McCall, PhD, Department of Specialty Medicine, Ohio University Heritage College of Osteopathic Medicine, Heritage Hall, 191 West Union St, Athens, OH 45701 (e-mail: mccallk@ohio.edu).

Supported in part by a National Institutes of Health, NIDDK grant (grant 1R15DK081192-01 to K.D.M.), the J.O. Watson Endowment for Diabetes Research, the Ohio University Heritage College of Osteopathic Medicine, and the John J. Kopchick Molecular and Cellular Biology/Translational Biomedical Sciences fund.

The authors declare no conflict of interest.

All data sets generated during and analyzed during the present study are not publicly available but are available from the corresponding author on reasonable request.

Copyright © 2022 The Author(s). Published by Wolters Kluwer Health, Inc. This is an open-access article distributed under the terms of the Creative Commons Attribution-Non Commercial-No Derivatives License 4.0 (CCBY-NC-ND), where it is permissible to download and share the work provided it is properly cited. The work cannot be changed in any way or used commercially without permission from the journal.

DOI: 10.1097/MPA.0000000000001960

University. Glucose measurements were conducted weekly using the FreeStyle Lite glucose monitoring system (Abbott Diabetes Care, Inc, Alameda, Calif). Blood glucose measurements were nonfasting and were consistently measured at the same time of day (ie, early morning approximately 8:00 A.M.). Diabetes was defined as blood glucose values greater than 240 mg/dL on consecutive days; however, no mice in this study were diabetic by the end point (ie, 8 weeks +3 days of age or 3 days after CVB4 infection). Eight-week-old female *Tlr3*^{+/+} and *Tlr3*^{-/-} NOD mice received an intraperitoneal injection of 5×10^5 plaque forming units of CVB4 (kindly provided by Dr Roger Loria, Virginia Commonwealth University).³⁵

Insulin Staining of Pancreatic Tissue

Harvested pancreata from 4-, 6-, and 8-week-old uninfected *Tlr3*^{+/+} and *Tlr3*^{-/-} NOD and uninfected and CVB4-infected *Tlr3*^{+/+} and *Tlr3*^{-/-} 8 weeks +3 days of age NOD mice underwent formalin-fixed paraffin embedded protocols and slides containing tissue sections were deparaffinized, rehydrated, and antigen retrieval using sodium citrate (10 mM, pH 6) was completed. Following the protocol provided from Abcam EXPOSE rabbit-specific horseradish peroxidase (HRP)/3,3'-diaminobenzidine detection kit (Abcam, Cambridge, Mass), tissues were incubated in a 1:1000 dilution of rabbit antimouse insulin antibody (Abcam). Goat antirabbit HRP-conjugated secondary antibody (from kit) was added directly onto the tissues followed by a 1:50 dilution of DAB plus chromogen (from kit) and a counterstain with hematoxylin. Slides were dehydrated after opposite order of the rehydration steps and mounted with permount and a coverslip (ThermoFisher, Carlsbad, Calif).

CD3 Immunostaining of Pancreatic Tissue

Slides of tissues were rehydrated following the same steps as insulin staining. Antigen retrieval using Proteinase K (Abcam) was followed by a 3% hydrogen peroxide block and protein block (either a 5% goat serum or 10% donkey serum, 1% BSA in PBS). Rabbit antimouse CD3 (1:200 dilution, Abcam) was added and incubated overnight at 4°C. Tissues were then incubated in goat antirabbit-specific HRP-conjugate (from EXPOSE kit) secondary antibody at a dilution of 1:500. For CD3 staining, a 1:50 dilution of DAB plus chromogen (from EXPOSE kit) was added followed by counterstain with hematoxylin, and slides were mounted as described above.

Insulinitis Scoring and Percent CD3⁺ T-Cell Infiltration of Islets

Sections of insulin-immunostained pancreas were assessed for insulinitis on Nikon Eclipse 80i microscope (Melville, NY) with Evolution MP color camera (Media Cybernetics, Rockville, Md) at 400× magnification and ranking of insulinitis for each islet was based on a previously described scale.²³ Sections of insulin-immunostained pancreas were assessed for percentage of immune cell infiltration using ImageJ Software Version 1.53e (National Institutes of Health, Rockville, Md).³⁶ Percent of immune cell infiltration was calculated by subtracting the area of insulin staining in the islet section from the total area of the islet section and then dividing by the total area of the islet section and multiplying by 100. An average of 28 islets per mouse were analyzed. CD3 immunohistochemical staining was done to confirm that the immune cell infiltration areas of the islets that were measured were CD3⁺ T cells.

Tissue Preparation for LCM of Islets

All equipment, including microtome, blades, water bath, brushes, and polyethylene naphthalate membrane (PEN-membrane) slides (Applied Biosystems, Foster City, Calif), was sprayed with RNase Away (ThermoFisher) before tissue sectioning. Tissue sections were

sliced at a 12- μ m thickness (separated by 36 μ m), deparaffinized, rehydrated, and stained with hematoxylin and eosin. Slides were air dried, followed by brief incubation on a hot plate and immediately taken to the Leica LMD6000 microscope (Buffalo Grove, Ill) for islet isolation as previously described.³⁷

RNA Extraction From Islets Isolated by LCM

To obtain sufficient RNA to run reverse transcription real-time polymerase chain reaction (RT-qPCR), islets were pooled from 3 to 4 different mice per group; thus, no statistical analysis can be performed. Because of islet pooling, the following modifications to the traditional delta-delta Ct analysis were made. The Livak and Schmittgen's delta-delta Ct method for one housekeeping gene (*Rn18s*) was used.³⁸ Delta Ct (Δ Ct) was calculated by subtracting the Ct of the housekeeping gene from the Ct of the gene of interest. Because the samples were pooled, no calibrator/reference sample was available to further calculate delta-delta Ct. $1/\Delta$ Ct provided a way to compare relative gene expression between groups. Thus, RT-qPCR results are represented as $1/\Delta$ Ct to compare relative gene expression between groups. Islet numbers ranged from 25 to 65/mouse. RNA extraction was performed using the RNeasy FFPE Kit (Qiagen, Hilden, Germany). RNA integrity and quantity were assessed using the Agilent 2100 Bioanalyzer (Santa Clara, Calif) at the Ohio University Genomics Facility.

cDNA Synthesis

cDNA was synthesized using Applied Biosystems High Capacity cDNA Reverse Transcription kit with RNase inhibitor (ThermoFisher) according to the manufacturer's instructions.

qPCR of Islet RNA

All cDNA was preamplified for target genes using TaqMan PreAmp Master Mix (ThermoFisher) with the following gene expression assays: *Cxcl10*, Mm00445235_m1; *Ill1b*, Mm00434228_m1; *Ifnb1*, Mm00439552_s1; *Tnfa*, Mm00443258_m1; *Tgfb1*, Mm01178820_m1; and all FAM labeled. cDNA preamplification consisted of 14 cycles of 95°C for 15 seconds, followed by 60°C for 4 minutes. Expression of the abovementioned genes was detected using TaqMan Gene Expression Master Mix (ThermoFisher) and gene expression assays previously mentioned. In addition, 18S ribosomal RNA (*Rn18s*, Mm03928990_g1; VIC labeled) was used as the housekeeping gene in duplex with each gene of interest. Each sample was run in duplicate on BioRad CFX384 Touch Real-Time PCR Detection System (Hercules, Calif). The PCR cycles were 40 cycles of 95°C for 15 seconds, followed by 60°C for 1 minute.

Statistical Analyses

Statistical analyses were performed using Statistica V13.3 software (Tibco, Palo Alto, Calif). Independent Student *t* tests or 1-way analyses of variance were used for comparisons. $P \leq 0.05$ was considered significant or as indicated.

RESULTS

Quantification of Insulinitis and CD3⁺ T-Cell Infiltration in Pancreatic Islets of Young Female *Tlr3*^{+/+} and *Tlr3*^{-/-} NOD Mice With Impact of CVB4 Infection in 8-Week-Old Mice 3 Days After Infection

Multiple previous studies have shown that 8 weeks is the age when *Tlr3*^{+/+} NOD mice have achieved a "critical threshold of insulinitis" (in approximately 30%–50% of mice) needed for the

CVB4 virus to trigger an acute acceleration of T1DM. We observed that *Tlr3*^{+/+} NOD mice exhibited significantly higher insulinitis scores at 8 weeks and significantly greater CD3⁺ T-cell infiltration of islets at ages 4 weeks and 8 weeks, compared with *Tlr3*^{-/-} NOD mice (Figs. 1A, B). At the critical age of 8 weeks, both *Tlr3*^{+/+} and *Tlr3*^{-/-} female NOD mice were infected with CVB4 and insulinitis scores and CD3⁺ T-cell infiltration of islets were assessed at 3 days after infection. Insulinitis scores and CD3⁺ T-cell infiltration in CVB4-infected *Tlr3*^{+/+} (Figs. 1A, B, red bars, *P* ≤ 0.001) and *Tlr3*^{-/-} (Figs. 1A, B, dashed black bar, *P* ≤ 0.001) female NOD mice roughly doubled in both groups at 3 days after CVB4 infection compared with the 8-week-old mice. Insulinitis scores and CD3⁺ T-cell infiltration of islets were again significantly (Figs. 1A, B, solid black bars, *P* ≤ 0.01 and *P* ≤ 0.001, respectively) higher in the *Tlr3*^{+/+} NOD mice compared with *Tlr3*^{-/-} NOD mice at 3 days after CVB4 infection.

Representative images of insulin and CD3⁺ immunohistochemical staining of pancreas preparations obtained from the *Tlr3*^{+/+} and *Tlr3*^{-/-} NOD mice at 8 weeks of age (ie, before CVB4 infection) are depicted (Figs. 1C, D, respectively; top rows). At 8 weeks of age, insulin immunostaining in islets from *Tlr3*^{+/+} NOD mice was lower than that in *Tlr3*^{-/-} NOD mice before CVB4 infection (Fig. 1C, top row). CD3⁺ T-cell infiltration of islets was significantly greater in the *Tlr3*^{+/+} NOD mice compared with *Tlr3*^{-/-} NOD mice at 8 weeks of age (Fig. 1B); the immunostaining pattern of CD3⁺ T-cell infiltration (insulinitis) in the islets obtained from *Tlr3*^{+/+} and *Tlr3*^{-/-} NOD mice at 8 weeks of age roughly matches the percentages of CD3⁺ T-cell infiltration (23% in *Tlr3*^{+/+} vs 15% *Tlr3*^{-/-} NOD mice) at 8 weeks of age (Fig. 1D, top row).

At 3 days after CVB4 infection, islet immunohistochemical staining revealed that islets are still intact in both cohorts and insulin

staining was still present in both *Tlr3*^{+/+} NOD mice and *Tlr3*^{-/-} NOD mice (Fig. 1C; bottom row). CD3⁺ T-cell infiltration was again higher in the *Tlr3*^{+/+} NOD mice and greater exocrine pancreatic inflammation is apparent in the *Tlr3*^{+/+} NOD mice compared with *Tlr3*^{-/-} NOD mice (Fig. 1D; bottom row) after CVB4 infection at 3 days.

Cytokine and Chemokine Expression in Islets of Uninfected and CVB4-Infected *Tlr3*^{+/+} and *Tlr3*^{-/-} NOD Mice

We next evaluated the expression of the key chemokine, *Cxcl10*, and cytokines (*Il1b*, *Ifnb1*, *Tnfa*, and *Tgfb1*) between the ages of 4 to 8 weeks during CD3⁺ T-cell infiltration (insulinitis) of islets isolated from uninfected and CVB4-infected female *Tlr3*^{+/+} and *Tlr3*^{-/-} NOD mice, as well as their expression 3 days after CVB4 infection (Figs. 2–6). Each of these factors has been shown previously to be involved in T1DM development.^{39–42} The current studies were performed to determine the influence of TLR3 on the expression of each of these genes during insulinitis between 4 and 8 weeks of age in female *Tlr3*^{+/+} and *Tlr3*^{-/-} NOD mice and determine how they each collectively or independently contribute to establishing the “critical threshold” of insulinitis at 8 weeks of age and what happens to these genes at 3 days after CVB4 infection. Moreover, this was done to determine whether these genes are involved in the acceleration of CVB4-induced diabetes observed in female *Tlr3*^{+/+} NOD mice or conversely the protection of female *Tlr3*^{-/-} NOD mice from CVB4-induced onset of diabetes observed 14 days after virus infection.²³

Cxcl10 expression in isolated islets obtained from uninfected female *Tlr3*^{+/+} NOD and *Tlr3*^{-/-} NOD mice was higher in the *Tlr3*^{+/+}

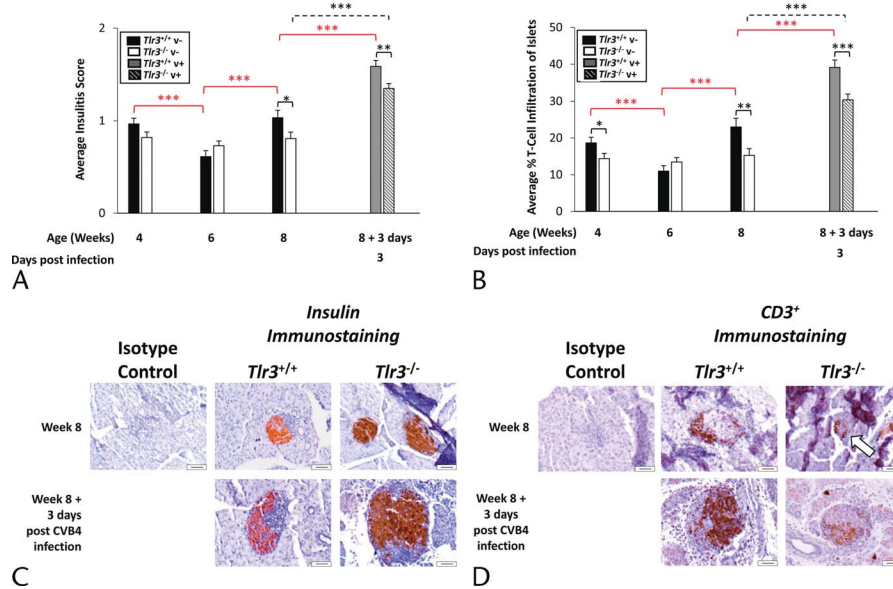


FIGURE 1. Uninfected and CVB4-infected *Tlr3*^{+/+} NOD mice have more severe insulinitis as well as elevated T-cell infiltration of pancreatic islets compared with *Tlr3*^{-/-} NOD mice. Pancreata from uninfected and CVB4-infected female *Tlr3*^{+/+} and *Tlr3*^{-/-} NOD mice were isolated and evaluated by immunohistochemistry. Insulinitis score and amount of immune cell infiltration of islets were assessed for individual islets from each mouse (an average of 28 islets/mouse were analyzed). A, Average insulinitis scores and (B) percent T-cell infiltration of islets for all mice within each group were calculated and represented. C and D, Examples of images of pancreas/islets stained for insulin (C) and CD3 (D) by immunohistochemistry and counterstained with hematoxylin and eosin that were used for assessment of insulinitis and T-cell infiltration of islets. Arrow in (D) is pointing at the small islet in the picture. All pictures are at 40× magnification. Scale bars are 50 μm. All data are expressed as means ± standard error of the mean (n = 5–11 mice/group). *P* values were calculated using a 1-way analysis of variance or Student *t* test where appropriate. **P* ≤ 0.05, ***P* ≤ 0.01, and ****P* ≤ 0.001. Red bars indicate differences between *Tlr3*^{+/+} groups at different time points as indicated, dashed black bars indicate differences between *Tlr3*^{-/-} groups at different time points as indicated, solid black bars indicate differences between *Tlr3*^{+/+} and *Tlr3*^{-/-} groups at the same time points as indicated. v-, no CVB4 infection; v+, CVB4 infection.

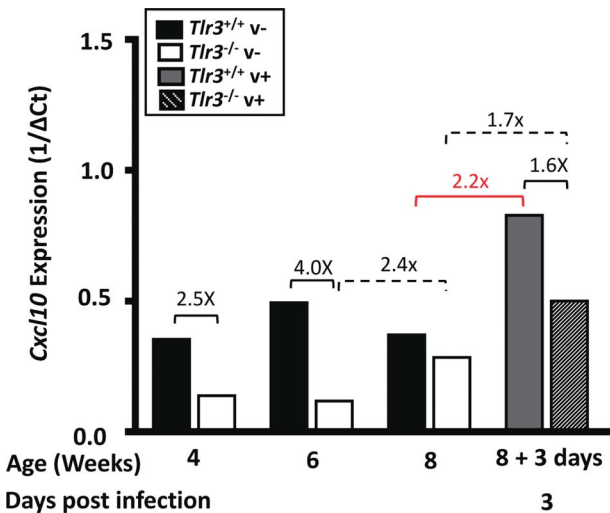


FIGURE 2. *Cxcl10* gene expression in islets of uninfected and CVB4-infected female *Tlr3*^{+/+} and *Tlr3*^{-/-} NOD mice. Multiple (25–65) individual islets from each female *Tlr3*^{+/+} and *Tlr3*^{-/-} NOD mouse (n = 3–4 mice/group) were isolated using laser capture microdissection, and then all islets from all mice/group (the total number of islets represented per group = 75–260) were pooled to isolate enough RNA for subsequent Taqman RT-qPCR analysis of *Cxcl10* gene expression. All data are represented as 1/ΔCt. Red bars indicate ≥1.5-fold change in gene expression between *Tlr3*^{+/+} groups at different time points as indicated, dashed black bars indicate ≥1.5-fold change in gene expression between *Tlr3*^{-/-} groups at different time points as indicated, and solid black bars indicate ≥1.5-fold change in gene expression between *Tlr3*^{+/+} and *Tlr3*^{-/-} groups at the same time points as indicated. Numbers above bars indicate the actual fold change in gene expression between indicated groups having a ≥1.5-fold change. v-, no CVB4 infection; v+, CVB4 infection.

NOD islets compared with *Tlr3*^{-/-} NOD islets between the age of 4 and 8 weeks with 6 weeks of age having the largest fold change (Fig. 2). *Cxcl10* expression in islets of *Tlr3*^{+/+} NOD mice increased dramatically 3 days after CVB4 infection (2.2-fold), whereas the *Cxcl10* expression in response to the CVB4 infection in islets of *Tlr3*^{-/-} NOD mice was less (1.7-fold) at 3 days after CVB4 infection compared with that in the *Tlr3*^{+/+} NOD mice (Fig. 2). Moreover, the *Cxcl10* expression was lower in the islets of the *Tlr3*^{-/-} NOD mice (1.6-fold) than that in the *Tlr3*^{+/+} NOD mice at 3 days after CVB4 infection (Fig. 2).

Il1b expression in islets of nonvirus-infected *Tlr3*^{+/+} NOD mice was highest at 4 weeks of age and greater than in *Tlr3*^{-/-} NOD mice at each age; however, expression did not appreciably increase between 4 and 8 weeks of age in either cohort of mice (ie, *Tlr3*^{+/+} and *Tlr3*^{-/-} NOD mice; Fig. 3). *Il1b* expression increased dramatically in isolated islets from both *Tlr3*^{+/+} and *Tlr3*^{-/-} NOD mice at 3 days after CVB4 infection (2.0- and 2.5-fold, respectively) and there was no appreciable difference in *Il1b* expression between *Tlr3*^{+/+} and *Tlr3*^{-/-} NOD mice at this time point (Fig. 3).

Islet *Ifnb1* expression was relatively low in both *Tlr3*^{+/+} and *Tlr3*^{-/-} NOD mice at 4 weeks of age, increased in both cohorts at 6 weeks of age, and was higher in the *Tlr3*^{-/-} NOD mice at 8 weeks of age compared with infected *Tlr3*^{+/+} (Fig. 4). After CVB4 infection, *Ifnb1* expression increased in islets of both cohorts of mice (Fig. 4, red and dashed black bars); however, response to the virus was almost twice as high (1.8-fold) in the *Tlr3*^{-/-} NOD mice at 3 days after CVB4 infection compared with *Tlr3*^{+/+} NOD mice (Fig. 4, solid black bar).

Islet expression of both *Tnfa* and *Tgfb1* were higher in islets of *Tlr3*^{+/+} NOD mice compared with that in islets of *Tlr3*^{-/-} NOD mice at 4 and 6 weeks of age; however, at 8 weeks of age, there were no appreciable differences in islet expression of either cytokine (Figs. 5, 6, respectively). At 3 days after CVB4 infection, the expression of *Tnfa* increased dramatically (Fig. 5, red and dashed black bars) and was essentially equivalent in islets from both the *Tlr3*^{+/+} and *Tlr3*^{-/-} NOD mice (Fig. 5). Similar to *Ifnb1* expression (Fig. 4), *Tgfb1* expression in response to CVB4 infection was greater (1.6-fold) in *Tlr3*^{-/-} NOD mice at 3 days after infection compared with *Tlr3*^{+/+} NOD mice (Fig. 6, solid black bar).

In short, islet expression of the cytokines, *Il1b*, *Ifnb1*, *Tnfa*, and *Tgfb1*, and the chemokine *Cxcl10* tended to be higher in islets of uninfected *Tlr3*^{+/+} NOD mice compared with islets of uninfected *Tlr3*^{-/-} NOD mice from 4 to 6 weeks of age (Figs. 2–6). By 8 weeks of age, islet expression of nearly all the genes was comparable in *Tlr3*^{+/+} and *Tlr3*^{-/-} NOD mice (Figs. 2–6), with the exception of *Ifnb1* which was more highly expressed (3.3-fold) in islets of uninfected *Tlr3*^{-/-} NOD mice relative to islets of age-matched, uninfected *Tlr3*^{+/+} NOD mice (Fig. 4). While CVB4 infection caused increases in islet expression of all genes evaluated at 3 days after CVB4 infection compared with their expression in islets of 8-week-old, uninfected mice (Figs. 2–6), *Cxcl10* was the only gene that was more highly expressed in islets of CVB4-infected *Tlr3*^{+/+} NOD mice (Fig. 2), a large percentage of which develop diabetes by 14 days after infection,²³ compared with islets of CVB4-infected *Tlr3*^{-/-} NOD mice, which do not develop diabetes by 14 days after infection.²³ However, *Ifnb1* and *Tgfb1*

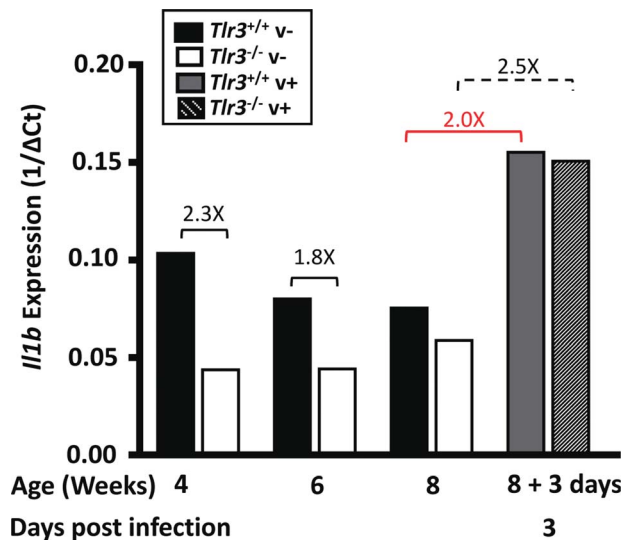


FIGURE 3. *Il1b* gene expression in islets of uninfected and CVB4-infected female *Tlr3*^{+/+} and *Tlr3*^{-/-} NOD mice. Multiple (25–65) individual islets from each female *Tlr3*^{+/+} and *Tlr3*^{-/-} NOD mouse (n = 3–4 mice/group) were isolated using laser capture microdissection, and then all islets from all mice/group (the total number of islets represented per group = 75–260) were pooled to isolate enough RNA for subsequent Taqman RT-qPCR analysis of *Il1b* gene expression. All data are represented as 1/ΔCt. Red bars indicate ≥1.5-fold change in gene expression between *Tlr3*^{+/+} groups at different time points as indicated, dashed black bars indicate ≥1.5-fold change in gene expression between *Tlr3*^{-/-} groups at different time points as indicated, and solid black bars indicate ≥1.5-fold change in gene expression between *Tlr3*^{+/+} and *Tlr3*^{-/-} groups at the same time points as indicated. Numbers above bars indicate the actual fold change in gene expression between indicated groups having a ≥1.5-fold change. v-, no CVB4 infection; v+, CVB4 infection.

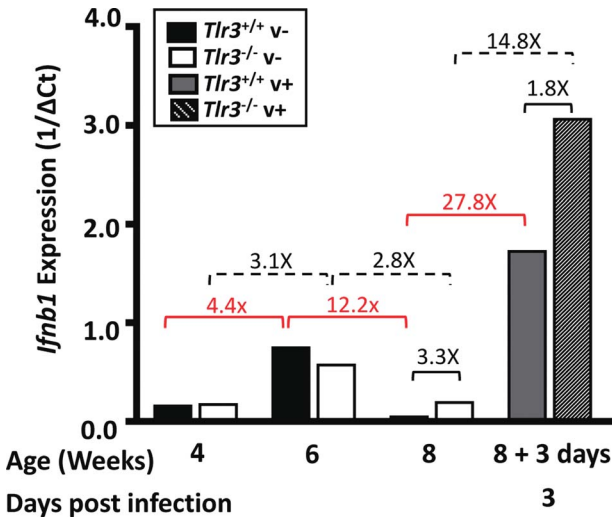


FIGURE 4. *Ifnb1* gene expression in islets of uninfected and CVB4-infected female *Tlr3*^{+/+} and *Tlr3*^{-/-} NOD mice. Multiple (25–65) individual islets from each female *Tlr3*^{+/+} and *Tlr3*^{-/-} NOD mouse (n = 3–4 mice/group) were isolated using laser capture microdissection, and then all islets from all mice/group (the total number of islets represented per group = 75–260) were pooled to isolate enough RNA for subsequent Taqman RT-qPCR analysis of *Ifnb1* gene expression. All data are represented as 1/ΔCt. Red bars indicate ≥1.5-fold change in gene expression between *Tlr3*^{+/+} groups at different time points as indicated, dashed black bars indicate ≥1.5-fold change in gene expression between *Tlr3*^{-/-} groups at different time points as indicated, and solid black bars indicate ≥1.5-fold change in gene expression between *Tlr3*^{+/+} and *Tlr3*^{-/-} groups at the same time points as indicated. Numbers above bars indicate the actual fold change in gene expression between indicated groups having a ≥1.5-fold change. v-, no CVB4 infection; v+, CVB4 infection.

expression was increased in islets of CVB4-infected, *Tlr3*^{-/-} NOD mice compared with islets of CVB4-infected *Tlr3*^{+/+} NOD mice (Figs. 4, 6, respectively).

DISCUSSION

Female NOD mice spontaneously develop an autoimmune, T-cell-mediated insulinitis, with gradual β-cell destruction/loss and onset of T1DM beginning at age approximately 15 weeks in a nonsterile environment, and by 25 weeks of age nearly 80% of the cohort will be diabetic.⁴³ Recently, the important role of NOD mice as an animal model in T1DM research has been reviewed.⁴⁴ Viruses and CVB4, in particular, have been investigated as principle triggers initiating, as well as accelerating, the onset of T1DM. Multiple investigations have demonstrated that CVB4 infection in *Tlr3*^{+/+} (ie, wild-type) female NOD mice can induce the rapid onset of diabetes within 2 weeks after infection; however, there is a “critical threshold” of spontaneous preexisting insulinitis (at 8–10 weeks of age),⁴ required for this CVB4 acceleration of T1DM to occur.^{4,17,23,26} However, *Tlr3*^{-/-} female NOD mice are protected from CVB4 acceleration of T1DM.²³ The results of these studies indicate that *Tlr3*^{+/+} female NOD mice have increased insulinitis and an increase in *Cxcl10*, *Il1b*, *Tnfa*, and *Tgfb1* expression between 4 and 6 weeks of age compared with *Tlr3*^{-/-} female NOD mice. Taken together, our data offer insight into how TLR3 contributes to the establishment of the “critical threshold of insulinitis” necessary for viral acceleration of T1DM.

Toll-like receptor 3 is one of a family of pattern recognition receptors also involved in the innate immune response, which

recognizes viral or endogenous dsRNA released by virus-damaged β cells. Toll-like receptor 3 activation and signaling results in the production of key cytokines and chemokines that are known to play a role in the pathogenesis of T1DM in the female NOD mouse; however, although present in islets by 2 weeks of age, and during the insulinitis, which occurs between 4 and 8 weeks of age, we previously demonstrated that CVB4 induction/acceleration of diabetes onset in female wild-type, *Tlr3*^{+/+}, NOD mice occurred after CVB4 infection at 8 weeks of age, yet similarly CVB4-infected *Tlr3*^{-/-} NOD mice are protected from CVB4-accelerated induction of diabetes at this age.²³ Furthermore, *Tlr3*^{+/+} NOD female mice demonstrate higher concentrations of CD4⁺ and CD8⁺ T cells at 14 days after CVB4 infection compared with *Tlr3*^{-/-} NOD mice.²³ This study demonstrates that between 4 and 8 weeks of age, islets isolated from female *Tlr3*^{+/+} NOD mice exhibit significantly greater islet inflammation (insulinitis [Fig. 1A] and T-cell infiltration [Fig. 1B]) than *Tlr3*^{-/-} NOD mice. Islet expression of the chemokine *Cxcl10* (Fig. 2) as well as the cytokines *Il1b* (Fig. 3), *Tnfa* (Fig. 5), and *Tgfb1* (Fig. 6) were also higher between 4 and 6 weeks of age in uninfected *Tlr3*^{+/+} NOD mice compared with islets of uninfected *Tlr3*^{-/-} NOD mice, yet by age 8 weeks, the earliest age at which the “critical threshold” for CVB4 acceleration of T1DM in the *Tlr3*^{+/+} NOD mice occurs, there was no appreciable differences in expression of these chemokines and cytokines between the 2 cohorts (Figs. 2–6). CXCL10 is a major contributor to insulinitis, as it is secreted from damaged β cells signaling dendritic cells, macrophages, and other T cells to sites of destruction.^{39,45,46} This

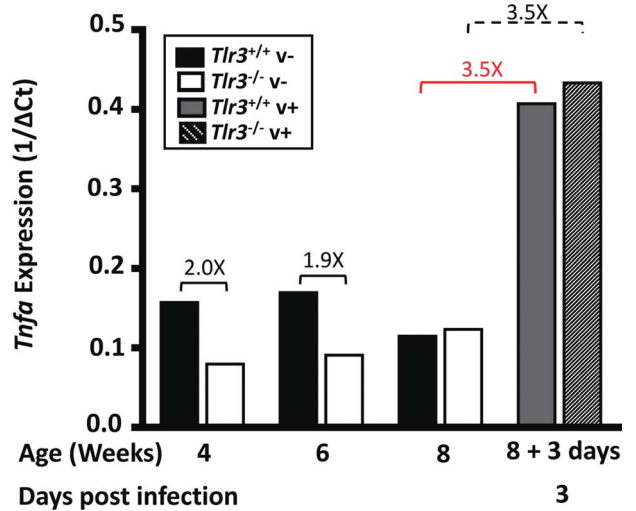


FIGURE 5. *Tnfa* gene expression in islets of uninfected and CVB4-infected female *Tlr3*^{+/+} and *Tlr3*^{-/-} NOD mice. Multiple (25–65) individual islets from each female *Tlr3*^{+/+} and *Tlr3*^{-/-} NOD mouse (n = 3–4 mice/group) were isolated using laser capture microdissection, and then all islets from all mice/group (the total number of islets represented per group = 75–260) were pooled to isolate enough RNA for subsequent Taqman RT-qPCR analysis of *Tnfa* gene expression. All data are represented as 1/ΔCt. Red bars indicate ≥1.5-fold change in gene expression between *Tlr3*^{+/+} groups at different time points as indicated, dashed black bars indicate ≥1.5-fold change in gene expression between *Tlr3*^{-/-} groups at different time points as indicated, and solid black bars indicate ≥1.5-fold change in gene expression between *Tlr3*^{+/+} and *Tlr3*^{-/-} groups at the same time points as indicated. Numbers above bars indicate the actual fold change in gene expression between indicated groups having a ≥1.5-fold change. v-, no CVB4 infection; v+, CVB4 infection.

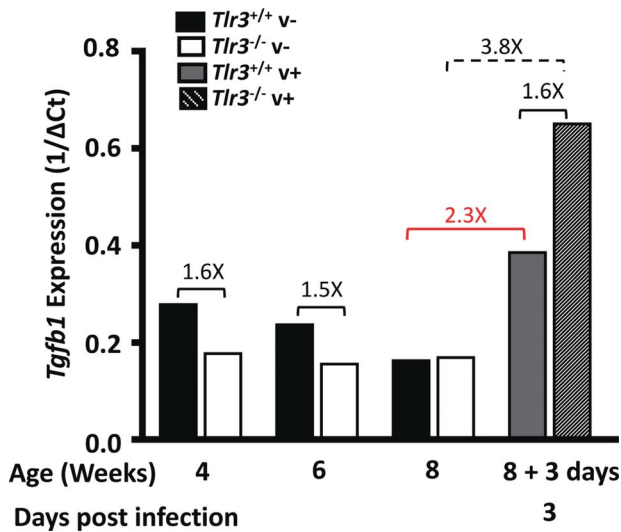


FIGURE 6. *Tgfb1* gene expression in islets of uninfected and CVB4-infected female *Tlr3*^{+/+} and *Tlr3*^{-/-} NOD mice. Multiple (25–65) individual islets from each female *Tlr3*^{+/+} and *Tlr3*^{-/-} NOD mouse (n = 3–4 mice/group) were isolated using laser capture microdissection, and then all islets from all mice/group (the total number of islets represented per group = 75–260) were pooled to isolate enough RNA for subsequent Taqman RT-qPCR analysis of *Tgfb1* gene expression. All data are represented as 1/ΔCt. Red bars indicate ≥1.5-fold change in gene expression between *Tlr3*^{+/+} groups at different time points as indicated, dashed black bars indicate ≥1.5-fold change in gene expression between *Tlr3*^{-/-} groups at different time points as indicated, and solid black bars indicate ≥1.5-fold change in gene expression between *Tlr3*^{+/+} and *Tlr3*^{-/-} groups at the same time points as indicated. Numbers above bars indicate the actual fold change in gene expression between indicated groups having a ≥1.5-fold change. v-, no CVB4 infection; v+, CVB4 infection.

increase in expression leading up to 8 weeks of age may aid in making the pancreatic microenvironment ideal for CVB4-accelerated T1DM to occur. In addition, interleukin 1 β and tumor necrosis factor α also contribute to this hostile environment by increasing inflammation and have been implicated in β -cell destruction and diabetes development.^{40,42,47–52} However, the increase in transforming growth factor- β may have been trying to counteract the proinflammatory cytokines by preventing self-reactive T cells from triggering T1DM onset^{41,51,53} as a decrease in transforming growth factor- β signaling has led to an acceleration of T1DM in NOD mice.⁴¹

Fifty percent of *Tlr3*^{+/+} NOD mice are known to develop diabetes by 14 days after CVB4 infection, whereas *Tlr3*^{-/-} NOD mice seem to be “protected” from CVB4-accelerated diabetes.²³ After CVB4 infection, *Tlr3*^{+/+} NOD mice histologically again exhibited greater insulinitis and T-cell infiltration at 3 days after infection than *Tlr3*^{-/-} NOD mice (Figs. 1A, B) with similar amounts of insulin staining (Fig. 1C). These data support our previous findings at 14 days after CVB4 infection and are likely to, at least in part, contribute to the 50% incidence of diabetes in the CVB4-infected *Tlr3*^{+/+} NOD mice and the protection of the *Tlr3*^{-/-} NOD mice that was observed previously.²³ Thus, this study agrees with our earlier studies demonstrating that CVB4-induced diabetes in the wild-type (ie, *Tlr3*^{+/+}) female NOD mice is TLR3 mediated²³ and show for the first time that TLR3 signaling enhances T-cell infiltration of young (4–8 weeks) islets along with expression of *Cxcl10* and cytokines *Il1b*, *Tnfa*, and *Tgfb1*, as *Tlr3*^{+/+} NOD mouse islets exhibit more T cells/greater insulinitis leading to the establishment of the “critical threshold” of insulinitis required for

CVB4-induced diabetes at 8 weeks of age. In addition, *Ifnb1* and *Tgfb1* levels increased dramatically in the *Tlr3*^{-/-} NOD mice in response to CVB4 compared *Tlr3*^{+/+} NOD mice, suggesting that they might actually be protective from viral-induced diabetes in this mouse model. Previous reports have shown that after viral infection, *IFN- β 1* expression is induced via IRF3 activation, through the TLR3 pathway.⁵⁴ Moreover, recent studies have shown that *IFN- β 1*^{-/-} mice were more susceptible to West Nile virus and had increased mortality, compared with *IFN- β 1*^{+/+} mice.^{55,56} Exactly how/why *Ifnb1* and *Tgfb1* expression increases in the absence of *Tlr3* in response to CVB4 is yet to be determined; however, one possibility may be due to compensation by other viral sensing pathways. Thus, although TLR3 is a key primary and major mediator of CVB4-induced T1DM in NOD mice, in its absence, there can be redundancy because some *Tlr3*^{-/-} NOD mice still develop T1DM. This redundancy is likely through dsRNA recognition by other pattern recognition receptors that sense cytoplasmic dsRNA such as retinoic acid-inducible gene 1 (RIG1) and/or melanoma differentiation associated factor 5.⁵⁷

As noted earlier, there was a drop in insulinitis and T-cell infiltration of islets from 4 to 6 weeks of age in *Tlr3*^{+/+} female NOD mice and a subsequent rise again at 8 weeks of age similar to the levels seen at 4 weeks of age (Figs. 1A, B, respectively). Insulinitis is considered a dynamic lesion at all stages of the disease with a continuous influx and efflux of immunocytes and progresses over time in response to immunologic and environmental influences.⁵⁸ Thus, the vacillation in insulinitis and T-cell infiltration from 4 to 8 weeks of age is likely a result of the fluctuation of different T-cell subtypes (and other CD3⁺ immunocytes) in and out of the islets of the younger female NOD mice (ie, up to 8 weeks of age) before the establishment of the critical threshold of insulinitis necessary for CVB4 to trigger T1DM in these mice (that typically occurs between 8–10 weeks of age), and the insulinitis then continues to increase over time. This fluctuation in insulinitis and T-cell infiltration of islets was not observed in the female *Tlr3*^{-/-} NOD mice, supporting the previously reported finding that *Tlr3*^{-/-} female NOD mice are protected from CVB4 acceleration of T1DM²³ and the results of the studies described herein indicating that *Tlr3*^{-/-} female NOD mice have decreased insulinitis and decreased *Cxcl10*, *Il1b*, *Tnfa*, and *Tgfb1* expression between 4 and 6 weeks of age, compared with *Tlr3*^{+/+} female NOD mice.

This study was not without limitations. Harvested islets had to be pooled for gene expression assays; thus, results are relative comparisons of gene expression rather than statistical comparisons. The NOD mouse model is ideal for studying T1DM, however, because of the heterogeneity of these animals, not all develop diabetes at the same time after CVB4 infection.

However, these studies are the first of their kind to (1) offer insight into the basic mechanisms by which TLR3 contributes to the “critical threshold” of insulinitis in female NOD mice, contributing to a better understanding of the natural progression of T1DM in these mice and providing a more detailed description of what constitutes the “critical threshold” of insulinitis and (2) describe the role of TLR3 in mediating CVB4-induced acceleration of T1DM in female NOD mice.

ACKNOWLEDGMENTS

The authors thank Dr Roger Loria (Virginia Commonwealth University) for providing the CVB4 for these studies, Dr Li Wen (Yale University) for providing the *Tlr3*^{-/-} NOD mice to establish a colony at Ohio University for these studies, and Molly Carrier for her assistance with immunostaining.

REFERENCES

- Devendra D, Eisenbarth GS. Interferon alpha—a potential link in the pathogenesis of viral-induced type 1 diabetes and autoimmunity. *Clin Immunol*. 2004;111:225–233.
- Yoon JW, Jun HS. Viruses cause type 1 diabetes in animals. *Ann N Y Acad Sci*. 2006;1079:138–146.
- Drescher KM, Kono K, Bopegamage S, et al. Coxsackievirus B3 infection and type 1 diabetes development in NOD mice: insulinitis determines susceptibility of pancreatic islets to virus infection. *Virology*. 2004;329:381–394.
- Serreze DV, Ottendorfer EW, Ellis TM, et al. Acceleration of type 1 diabetes by a coxsackievirus infection requires a preexisting critical mass of autoreactive T-cells in pancreatic islets. *Diabetes*. 2000;49:708–711.
- Horwitz MS, Bradley LM, Harbertson J, et al. Diabetes induced by Coxsackie virus: initiation by bystander damage and not molecular mimicry. *Nat Med*. 1998;4:781–785.
- Horwitz MS, Ilic A, Fine C, et al. Coxsackieviral-mediated diabetes: induction requires antigen-presenting cells and is accompanied by phagocytosis of beta cells. *Clin Immunol*. 2004;110:134–144.
- Horwitz MS, Fine C, Ilic A, et al. Requirements for viral-mediated autoimmune diabetes: beta-cell damage and immune infiltration. *J Autoimmun*. 2001;16:211–217.
- Tracy S, Drescher KM, Jackson JD, et al. Enteroviruses, type 1 diabetes and hygiene: a complex relationship. *Rev Med Virol*. 2010;20:106–116.
- Dotta F, Censini S, van Halteren AG, et al. Coxsackie B4 virus infection of beta cells and natural killer cell insulinitis in recent-onset type 1 diabetic patients. *Proc Natl Acad Sci U S A*. 2007;104:5115–5120.
- Coppieters KT, Boettler T, von Herrath M. Virus infections in type 1 diabetes. *Cold Spring Harb Perspect Med*. 2012;2:a007682.
- Gale EA. The rise of childhood type 1 diabetes in the 20th century. *Diabetes*. 2002;51:3353–3361.
- Banatvala JE, Bryant J, Schernthaner G, et al. Coxsackie B, mumps, rubella and cytomegalovirus specific IgM responses in patients with juvenile-onset insulin-dependent diabetes mellitus in Britain, Austria, and Australia. *Lancet*. 1985;325:1409–1412.
- Hindersson M, Elshebani A, Om A, et al. Simultaneous type 1 diabetes onset in mother and son coincident with an enteroviral infection. *J Clin Virol*. 2005;33:158–167.
- Mäkelä M, Vaarala O, Hermann R, et al. Enteral virus infections in early childhood and an enhanced type 1 diabetes-associated antibody response to dietary insulin. *J Autoimmun*. 2006;27:54–61.
- Jäidane H, Hober D. Role of coxsackievirus B4 in the pathogenesis of type 1 diabetes. *Diabetes Metab*. 2008;34:537–548.
- Oikarinen S, Martiskainen M, Tauriainen S, et al. Enterovirus RNA in blood is linked to the development of type 1 diabetes. *Diabetes*. 2011;60:276–279.
- Serreze DV, Wasserfall C, Ottendorfer EW, et al. Diabetes acceleration or prevention by a coxsackievirus B4 infection: critical requirements for both interleukin-4 and gamma interferon. *J Virol*. 2005;79:1045–1052.
- Atkinson MA, Eisenbarth GS. Type 1 diabetes: new perspectives on disease pathogenesis and treatment. *Lancet*. 2001;358:221–229.
- Filippi C, von Herrath M. How viral infections affect the autoimmune process leading to type 1 diabetes. *Cell Immunol*. 2005;233:125–132.
- Stene LC, Oikarinen S, Hyöty H, et al. Enterovirus infection and progression from islet autoimmunity to type 1 diabetes: the Diabetes and Autoimmunity Study in the Young (DAISY). *Diabetes*. 2010;59:3174–3180.
- Friman G, Fohlman J, Frisk G, et al. An incidence peak of juvenile diabetes. Relation to Coxsackie B virus immune response. *Acta Paediatr Scand Suppl*. 1985;320:14–19.
- Ylipaasto P, Klingel K, Lindberg AM, et al. Enterovirus infection in human pancreatic islet cells, islet tropism in vivo and receptor involvement in cultured islet beta cells. *Diabetologia*. 2004;47:225–239.
- McCall KD, Thuma JR, Courreges MC, et al. Toll-like receptor 3 is critical for coxsackievirus B4-induced type 1 diabetes in female NOD mice. *Endocrinology*. 2015;156:453–461.
- Jun HS, Yoon JW. A new look at viruses in type 1 diabetes. *Diabetes Metab Res Rev*. 2003;19:8–31.
- Orchard TJ, Becker DJ, Atchison RW, et al. The development of type 1 (insulin-dependent) diabetes mellitus: two contrasting presentations. *Diabetologia*. 1983;25:89–92.
- Tracy S, Drescher KM, Chapman NM. Enteroviruses and type 1 diabetes. *Diabetes Metab Res Rev*. 2011;27:820–823.
- Takeda K, Akira S. TLR signaling pathways. *Semin Immunol*. 2004;16:3–9.
- Matsumoto M, Funami K, Tanabe M, et al. Subcellular localization of toll-like receptor 3 in human dendritic cells. *J Immunol*. 2003;171:3154–3162.
- Dogusan Z, Garcia M, Flamez D, et al. Double-stranded RNA induces pancreatic beta-cell apoptosis by activation of the toll-like receptor 3 and interferon regulatory factor 3 pathways. *Diabetes*. 2008;57:1236–1245.
- Matsumoto M, Funami K, Tatematsu M, et al. Assessment of the toll-like receptor 3 pathway in endosomal signaling. *Methods Enzymol*. 2014;535:149–165.
- Vercammen E, Staal J, Beyaert R. Sensing of viral infection and activation of innate immunity by toll-like receptor 3. *Clin Microbiol Rev*. 2008;21:13–25.
- Wong FS, Hu C, Zhang L, et al. The role of toll-like receptors 3 and 9 in the development of autoimmune diabetes in NOD mice. *Ann N Y Acad Sci*. 2008;1150:146–148.
- Yamamoto M, Sato S, Hemmi H, et al. Role of adaptor TRIF in the MyD88-independent toll-like receptor signaling pathway. *Science*. 2003;301:640–643.
- Perales-Linares R, Navas-Martin S. Toll-like receptor 3 in viral pathogenesis: friend or foe? *Immunology*. 2013;140:153–167.
- Webb SR, Loria RM, Madge GE, et al. Susceptibility of mice to group B coxsackie virus is influenced by the diabetic gene. *J Exp Med*. 1976;143:1239–1248.
- Schneider CA, Rasband WS, Eliceiri KW. NIH image to ImageJ: 25 years of image analysis. *Nat Methods*. 2012;9:671–675.
- Szulawski R, Nakazawa M, McCall KD, et al. Laser capture microdissection tailored to type 1 diabetes mellitus research. *Biotechniques*. 2016;60:293–298.
- Livak KJ, Schmittgen TD. Analysis of relative gene expression data using real-time quantitative PCR and the 2^{-ΔΔCT} method. *Methods*. 2001;25:402–408.
- Ahmadi Z, Arababadi MK, Hassanshahi G. CXCL10 activities, biological structure, and source along with its significant role played in pathophysiology of type 1 diabetes mellitus. *Inflammation*. 2013;36:364–371.
- Amrani A, Verdaguer J, Thiessen S, et al. IL-1alpha, IL-1beta, and IFN-gamma mark beta cells for Fas-dependent destruction by diabetogenic CD4(+) T lymphocytes. *J Clin Invest*. 2000;105:459–468.
- Ishigame H, Zenewicz LA, Sanjabi S. Excessive Th1 responses due to the absence of TGF-β signaling cause autoimmune diabetes and dysregulated Treg cell homeostasis. *Proc Natl Acad Sci*. 2013;110:6961–6966.
- Pop SM, Wong CP, Culton DA, et al. Single cell analysis shows decreasing FoxP3 and TGFbeta1 coexpressing CD4+CD25+ regulatory T cells during autoimmune diabetes. *J Exp Med*. 2005;201:1333–1346.
- Kikutani H, Makino S. The murine autoimmune diabetes model: NOD and related strains. *Adv Immunol*. 1992;51:285–322.
- Chen YG, Mathews CE, Driver JP. The role of NOD mice in type 1 diabetes research: lessons from the past and recommendations for the future. *Front Endocrinol (Lausanne)*. 2018;9:51.

45. Paroni F, Domsgen E, Maedler K. CXCL10- a path to β -cell death. *Islets*. 2009;1:256–259.
46. Eizirik DL, Colli ML, Ortis F. The role of inflammation in insulinitis and beta-cell loss in type 1 diabetes. *Nat Rev Endocrinol*. 2009;5:219–226.
47. Gregori S, Giarratana N, Smiroldo S, et al. Dynamics of pathogenic and suppressor T cells in autoimmune diabetes development. *J Immunol*. 2003; 171:4040–4047.
48. Dahlén E, Dawe K, Ohlsson L, et al. Dendritic cells and macrophages are the first and major producers of TNF-alpha in pancreatic islets in the nonobese diabetic mouse. *J Immunol*. 1998;160:3585–3593.
49. Graser RT, DiLorenzo TP, Wang F, et al. Identification of a CD8 T cell that can independently mediate autoimmune diabetes development in the complete absence of CD4 T cell helper functions. *J Immunol*. 2000;164: 3913–3918.
50. Lehuen A, Diana J, Zaccone P, et al. Immune cell crosstalk in type 1 diabetes. *Nat Rev Immunol*. 2010;10:501–513.
51. Oh SA, Li MO. TGF- β : guardian of T cell function. *J Immunol*. 2013;191: 3973–3979.
52. Aribi M, Moulessehoul S, Kendouci-Tani M, et al. Relationship between interleukin-1beta and lipids in type 1 diabetic patients. *Med Sci Monit*. 2007;13:CR372–CR378.
53. Li MO, Flavell RA. TGF- β : a master of all T cell trades. *Cell*. 2008; 134:392–404.
54. Bourdon M, Manet C, Montagutelli X. Host genetic susceptibility to viral infections: the role of type I interferon induction. *Genes Immun*. 2020;21: 365–379.
55. Lazear HM, Pinto AK, Vogt MR, et al. Beta interferon controls West Nile virus infection and pathogenesis in mice. *J Virol*. 2011;85:7186–7194.
56. Deonarain R, Alcamí A, Alexiou M, et al. Impaired antiviral response and alpha/beta interferon induction in mice lacking beta interferon. *J Virol*. 2000;74:3404–3409.
57. Takeuchi O, Akira S. Pattern recognition receptors and inflammation. *Cell*. 2010;140:805–820.
58. Magnuson AM, Thurber GM, Kohler RH, et al. Population dynamics of islet-infiltrating cells in autoimmune diabetes. *Proc Natl Acad Sci U S A*. 2015;112:1511–1516.